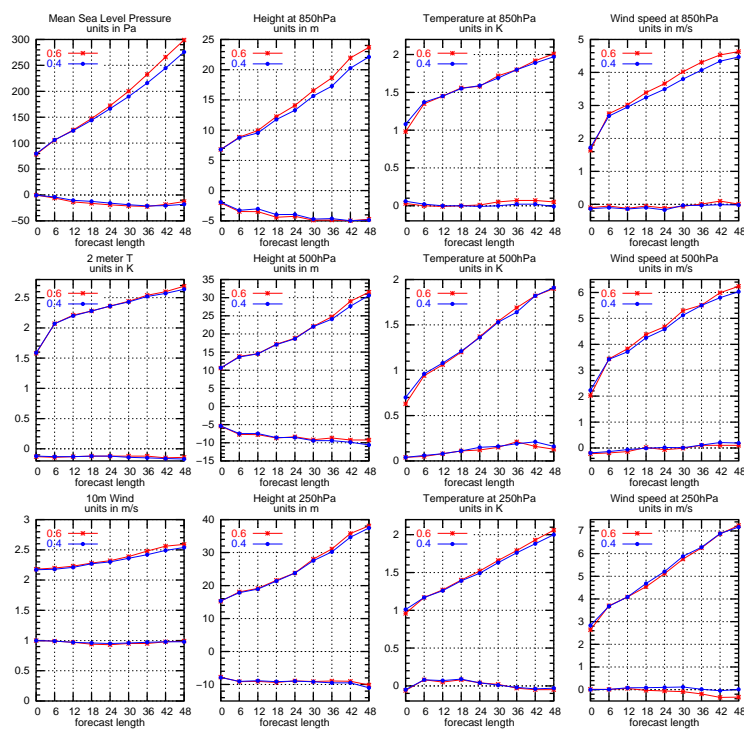


Technical Report 05-10

The DMI-HIRLAM Upgrade in May 2005

Xiaohua Yang, Maryanne Kmit, Bent Hansen Sass, Bjarne Amstrup, Karina Lindberg, Claus Petersen, Ulrik Korsholm, Niels Woetmann Nielsen





Colophone

Serial title:

Technical Report 05-10

Title:

The DMI-HIRLAM Upgrade in May 2005

Subtitle:

Authors:

Xiaohua Yang, Maryanne Kmit, Bent Hansen Sass, Bjarne Amstrup, Karina Lindberg, Claus Petersen, Ulrik Korsholm, Niels Woetmann Nielsen

Other Contributors:

Responsible Institution:

Danmarks Meteorologiske Institut

Language:

English

Keywords:

DMI-HIRLAM, Upgrade, 2005

Url:

www.dmi.dk/dmi/tr05-10

ISSN:

1399-1388

ISBN:

Version:

Website:

www.dmi.dk

Copyright:

Danish Meteorological Institute



Contents

Colophone	2
Abstract	4
Resume	4
Introduction	5
Surface analysis	5
Upper air analysis	8
Forecast model	12
Summary	17
Acknowledgment	19
References	20
Appendix: Operational schedule	21
Contact	22
Previous reports	22



Abstract

This report describes the May 2005 upgrade of DMI's operational forecast system DMI-HIRLAM and results of numerical experiments.

Resume

Denne rapport beskriver ændringerne i maj 2005 opgraderingen af DMIs operationelle prognosesystem, DMI-HIRLAM, og viser resultater fra nogle numeriske tests lavet i forbindelse hermed.

Introduction

An upgrade of DMI's operational forecast system, DMI-HIRLAM, has been carried out in late May 2005. The upgrade includes changes to source code and run-scripts of various components of DMI-HIRLAM. For the surface analysis, the Ocean & Sea Ice SAF (Satellite Application Facility) (OSI-SAF) is now included for assimilation of sea surface temperature (SST). The execution of the surface analysis, ISBA (Integrated Soil Biosphere Atmosphere), is now done on a full NEC SX-6 node with 8 processors using OpenMP, instead of using a single processor in the previous suite. The upper air analysis, 3D-VAR, is upgraded to the latest reference HIRLAM analysis code, HIRVDA 6.3.6. In addition, a reduced scaling of the background error standard deviation with a value of 0.4 for p_s , T , ageostrophic u and v is used instead of the previous value of 0.6. The new suite adds assimilation of Meteosat-8 AMV (Atmospheric Motion Vectors) wind data. In order to better utilize the computing resources, the 3D-VAR analysis is now performed on multi-nodes with MPI parallelization, as compared to the previous one with a single node and OpenMP option. For the forecast model, the interpolation scheme in the Semi-Lagrangian advection is upgraded to SETTLS (Stable Extrapolation Two-Time-level Scheme) based on McDonald's implementation, and a tuning of turbulence (CBR (Cuxart, Bougeault, Redelsperger)) and condensation (STRACO (Soft TRAnSition CONDensation)) schemes has been introduced. The upgrade also included a bug correction on radiation code to take into account correctly the cloud absorption for short wave radiation. In addition, the recent proposal by Sander Tjmm (2005) on modified specification about monthly leaf area index (LAI), vegetation index (VEGI) and a reduced stomatal resistance has been implemented. In addition to these changes, the experimental suite of high resolution model domain covering southern Greenland at 0.05 degree resolution, is now formally incorporated into the operational suite.

This report describes primarily the individual components of the upgrades and experiment results validating the updates, either individually or combined. The meteorological performance of the upgraded suites has been validated positively with T15 and S05 for historical episodes as well as in real-time parallel runs. The new suite is found to have brought an overall improvement in precipitation forecast, in particular in terms of reduced occurrence of severe false alarm and severe under-prediction cases. For spring season the new suite provides significant improvement on the previous tendency of negative surface moisture bias and positive surface temperature bias. For winter period the model prediction of synoptic development (e.g. mean sea level pressure and upper level heights) has been improved. The suite has a slight increase in positive surface wind bias. A summary of additional results of numerical experiments using the final implemented new DMI-HIRLAM is scheduled to be presented in an accompanying report.

Surface analysis

Assimilation of Ocean & Sea Ice SAF data

Until recently the main information source for the sea surface temperature (SST) in the DMI-HIRLAM system was the SST fields received twice daily from ECMWF at 0.5 degree resolution, supplemented by a less dense coverage of ship observations, (see more details in Yang et al. (2005)). In this upgrade, satellite observation retrievals from the Ocean & Sea Ice SAF (OSI-SAF) data (see <http://www.osi-saf.org/> for further information about the data production) has been added into the input data for the surface SST analysis in order to have the newest available data in use and also to obtain the higher resolution field. However, the typical number of data points in the data provided by OSI-SAF is very large and therefore some thinning is done by making very simple "super-observations": The data within squared boxes of size $0.2^\circ \times 0.2^\circ$ are averaged and used as one simple observation in the center of the box. Furthermore, the data are also screened by first

running through the data and making average values and standard deviation values when 2 or more observations are in a given box. Then, in the second run through the data, the data are rejected if they deviate more than 1.5 standard deviations and at least 1 K from the mean value of the observations in the box. The left over data then make a new mean value for the box to be used in the surface analysis.

The OSI-SAF SST data from satellite retrieval is introduced into the surface analysis system in the form of special SST observations in ASCII. This involves some minor modification to the source code in HIRLAM's surface analysis module.

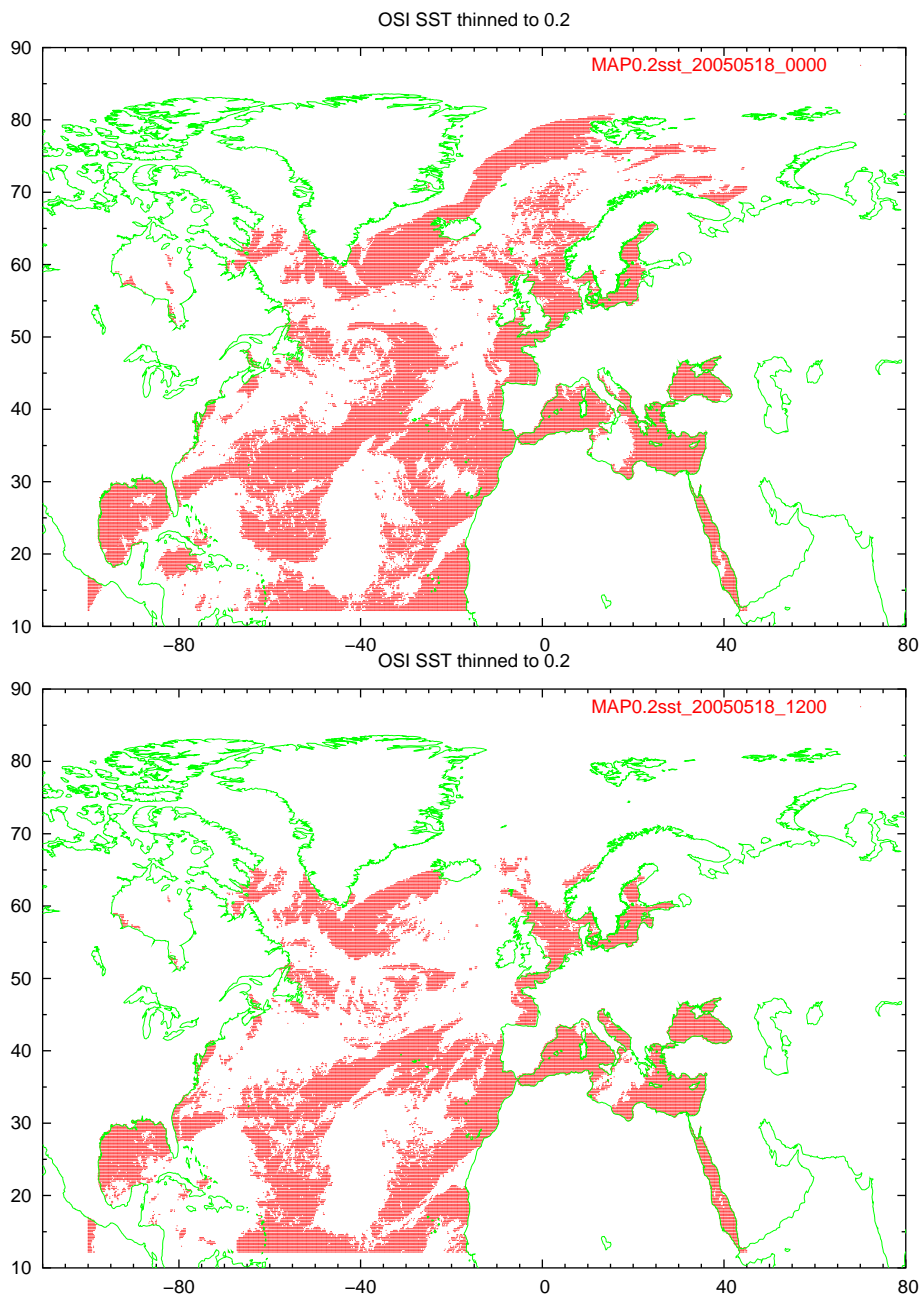


Figure 1: SST data coverage with the composite data set from OSI-SAF, for 00 UTC (upper panel) and 12 UTC (down) May 18 2005. The data has been thinned to a resolution of 0.2 degree.

Figure 1 illustrates, e.g., the thinned OSI-SAF SST data coverage over the T15 domain for 00 and 12 UTC, May 18, 2005. As shown in the figure, the horizontally thinned observation data provides a good coverage over the water fractions (ocean and lakes) around Europe except for areas with cloud cover, easily distinguishable from the data holes over bodies of water in Figure 1.

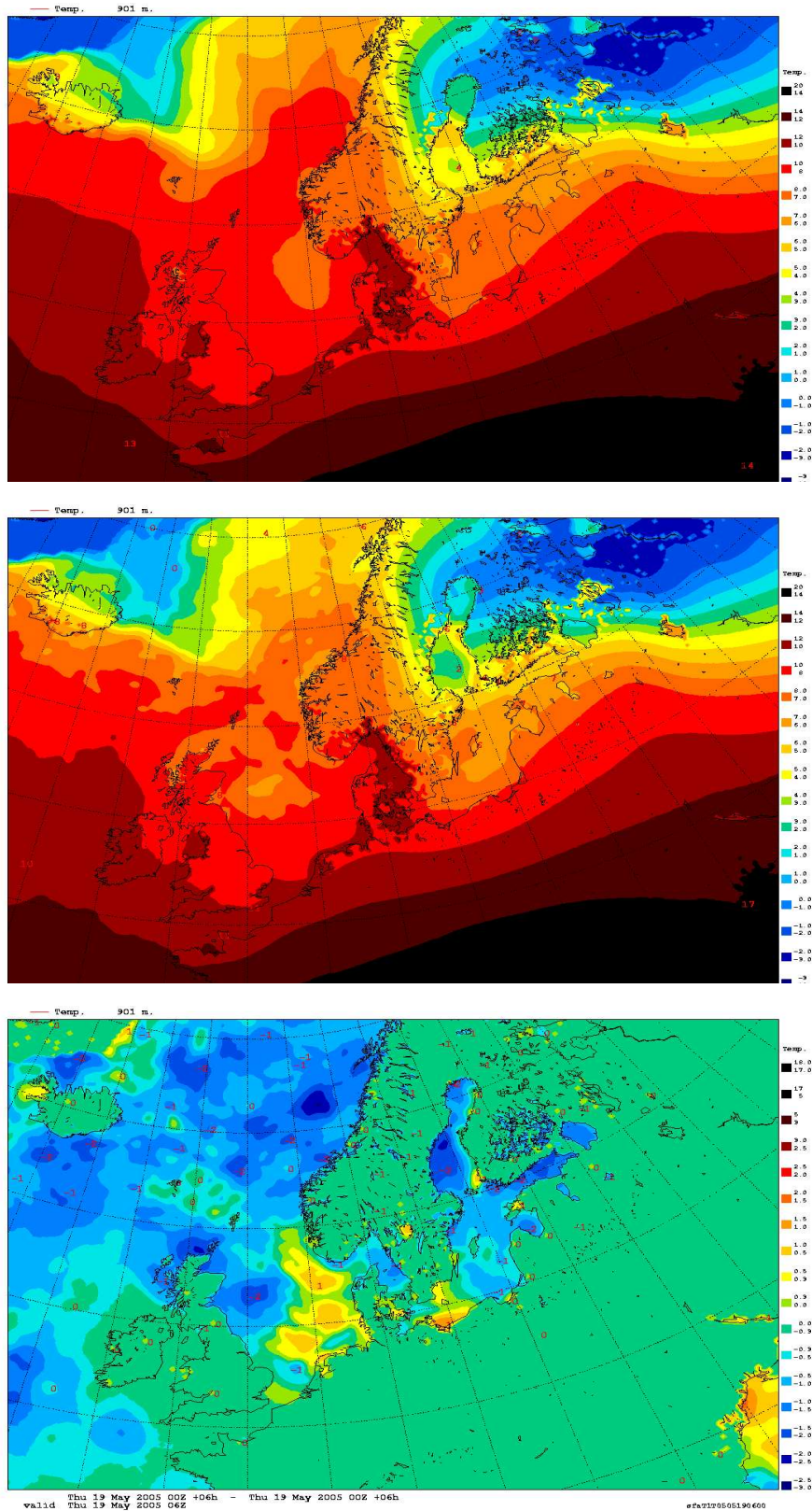


Figure 2: SST analysis for the area around Denmark at 06 UTC, May 19, 2005, with a) the previous operational DMI-HIRLAM-T15, upper panel; b) the new DMI-HIRLAM-T15 using additional information of OSI-SAF data, middle panel. The plot in the lowest panel shows the difference of the two with a maximum value of around 2°C.

The OSI SAF provides high resolution SST observations in both the temporal and spatial dimensions, adding more details to the existing surface SST analysis. Figure 2 shows, as an example, the SST analysis increment for the assimilation cycle on 06 UTC, May 19, 2005 on the T15 domain, comparing results with and without OSI SAF SST data. The one with OSI SAF SST is seen to have more features on finer scales.

The thinned OSI SAF SST data is introduced into the surface analysis module in the form of a pseudo SST observation and it amounts to around 40000 data points per assimilation cycle on the T15 domain. Compared to the previous SST analysis scheme (Yang et al., 2005), this is a dramatic change since so far only a limited number of ship observations (in 100s) is used. The major increase in the assimilated SST observation data has a significant consequence on the computation time of the SST analysis which employs a successive correction method (SC). To solve the efficiency problem, a minor change in the source code has been made to activate the OpenMP option, which enables execution of the surface analysis on multiple NEC-SX6 processors instead of on a single processor as before. Using 8 NEC-SX6 processors, the T15 surface analysis can now be finished within 3 to 4 minutes.

Upper air analysis

The recent HIRLAM 3D-VAR code release, HIRVDA 6.3.6, has been implemented in the operational suite. Compared to the HIRVDA version used in the earlier operational suite (equivalent to 6.3.2), most of changes in HIRVDA 6.3.6 are for non-standard options and thus do not have meteorological consequence for DMI-HIRLAM. One exception to this is the new modules in 6.3.6 which facilitates assimilation of the geostationary Meteosat-8 AMV wind data, see below. In connection with the upgrade, several new features or modifications have been tested in DMI-HIRLAM. These include the testing and tuning of background error statistics, the assimilation of AMV wind data, and running of 3D-VAR analysis on multi NEC-SX6 nodes using MPI.

Tuning of structure function scaling

In the initial implementation of HIRLAM 3D-VAR, the background error covariance matrices were derived from three winter months of the SMHI operational forecasts at 0.4 degree horizontal resolution and 31 vertical levels, applying the so-called NMC method with the analytical balance approach (Gustafsson et al., 2001). A scaling factor of approximately 0.6 was selected after tuning experiments. In addition, a seasonal dependence was added based on statistical analysis of innovation vectors (Lindskog, 2000). Later, in connection with the change of the vertical structure from 31 to 40 levels, the standard deviations of the background error for control parameters of surface pressure (p_s), ageostrophic winds (u_{ag} and v_{ag}), temperature (T) and specific humidity were interpolated to the new vertical levels.

In this work, a gross tuning of the scaling constants of the structure functions has been tested. The exercise is motivated by the operational experiences at several HIRLAM centers (DMI, SMHI, FMI, etc.) in recent years, revealing a general tendency to weight too heavily, in the 3D-VAR analyses, the observations over the backgrounds. This phenomenon has often been manifested in the behavior of the observation verification for HIRLAM forecasts, i.e., an initial good fit at the analysis time, followed thereafter by a rapidly decreasing skill along the forecast lead time¹.

Figure 4 shows observation verification results from a parallel assimilation experiment comparing

¹The fact with a relatively too large specified background error has also been confirmed in the recent diagnostic studies of the analysis error statistics in DMI-HIRLAM as well as in operational models at SMHI and FMI, see Navascués et al. (2006)

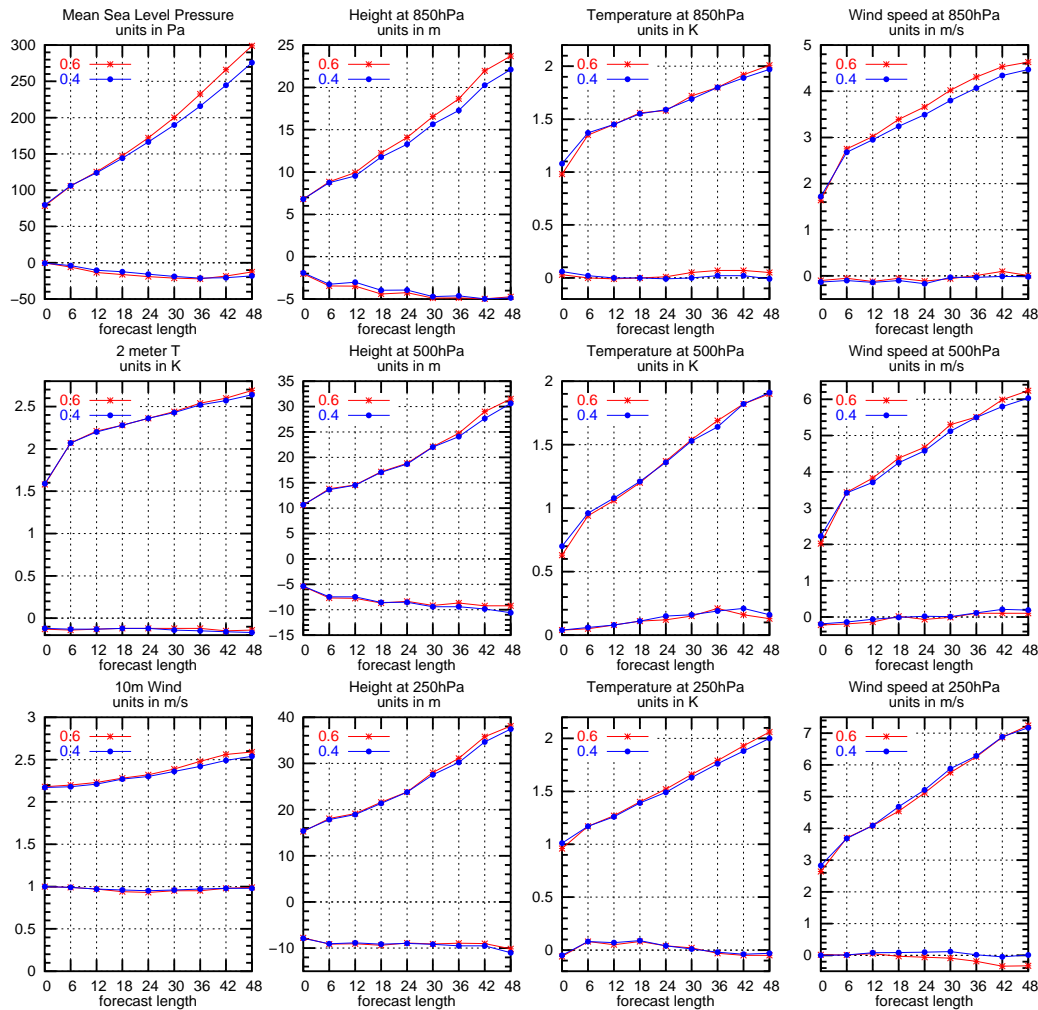


Figure 3: Observation verification scores (rms and bias validated against the EWGLAM station list) of key parameters averaged for forecasts with the 3D-VAR analysis using the interpolated SMHI 31-level background error structure function, with a scaling factor of a) 0.6 for p_s , u_{ag} , v_{ag} and T , and 0.8 for q , (in red); b) 0.4 for p_s , u_{ag} , v_{ag} and T , and 0.6 for q , (in blue). The test period is between Jan 15 and Jan 31, 2002. Note the forecast system used in this test is the reference HIRLAM 6.3.6 on the reference RCR grid with 0.2 degree resolution.

the use of a scale factor of 0.4 against 0.6, the latter being the current default values in both Reference HIRLAM and DMI-HIRLAM, using the reference structure functions. The results indicate a significant sensitivity of the forecast scores to the scaling of the background errors in the 3D-VAR analysis, with the runs using 0.4 being significantly better in rms values of key parameters such as mslp and several upper air parameters.

Ideally, background error statistics and their tuning should be made using information from the NWP suite in use. Over the past few years, efforts have been made at DMI to derive the background error structure functions from the archived T15 forecasts using the NMC method with the analytical balance approach. This has been motivated by a desire to derive the structure function which enable higher resolution 3D-VAR analysis increments (i.e., at T15's own resolution) and to obtain the background error structure functions from the current local forecasting system. In connection with this upgrade, parallel tests validating a recently derived structure function from archived T15 forecasts have been made, and the results so far are however mixed in terms of observation verification. In the initial test using the recent reference HIRLAM system on the T15 domain, the

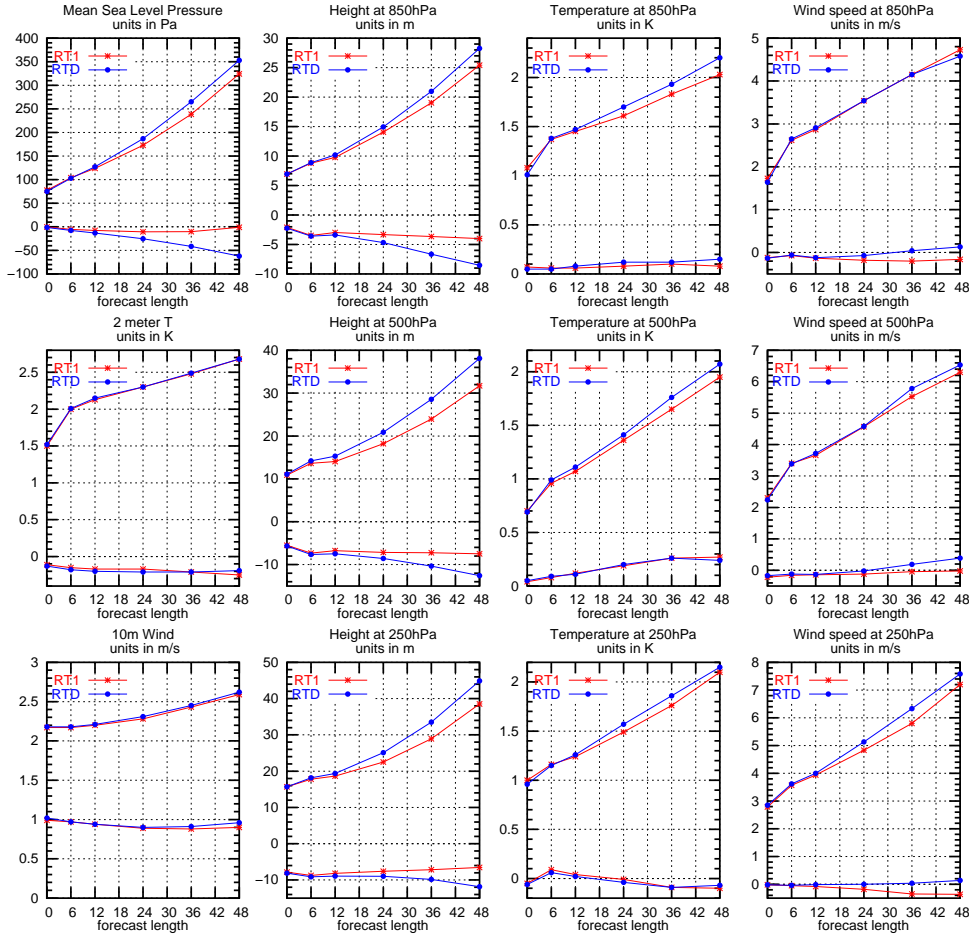


Figure 4: Observation verification scores of key parameters averaged for forecasts with 3D-VAR analyses using a) interpolated SMHI 31-level background error structure functions, with a scaling factor of 0.4 for p_s , u_{ag} , v_{ag} and T , and 0.6 for q , (in red), and b) T15 structure function with a scaling factor of 0.6 for p_s , T , q and 0.3 for u_{ag} and v_{ag} , (in blue). The test period is between Jan 15 and Jan 31, 2002. Note that the forecast system used in this test is the reference HIRLAM 6.3.6 but on the T15 grid with 0.15 degree resolution.

Table 1: Observation error standard deviations for AMV wind

Pressure (hPa)	1000	850	700	500	400	300	250	200
u/v (m/s)	2.00	2.00	2.00	2.45	3.10	3.60	3.80	3.80
Pressure (hPa)		150	100	70	50	30	20	10
u/v (m/s)		5.00	5.00	5.00	5.00	5.00	5.00	5.70

observation verification scores for the runs with T15 structure functions is significantly worse than those with the original structure function, see Figure 4. The reason for this is not entirely obvious, but one contributing factor could be that the model systems used to derive the T15 structure functions and for the experiments are not the same. On the other hand, a two week assimilation test for the same period, using DMI-HIRLAM, do show comparable results between the two versions, see Figure 5.

Based on the above experimental results, a reduced scaling-factor, 0.4, for the key analysis parameters, has been chosen in the new operational suite, while the reference structure functions are still used.

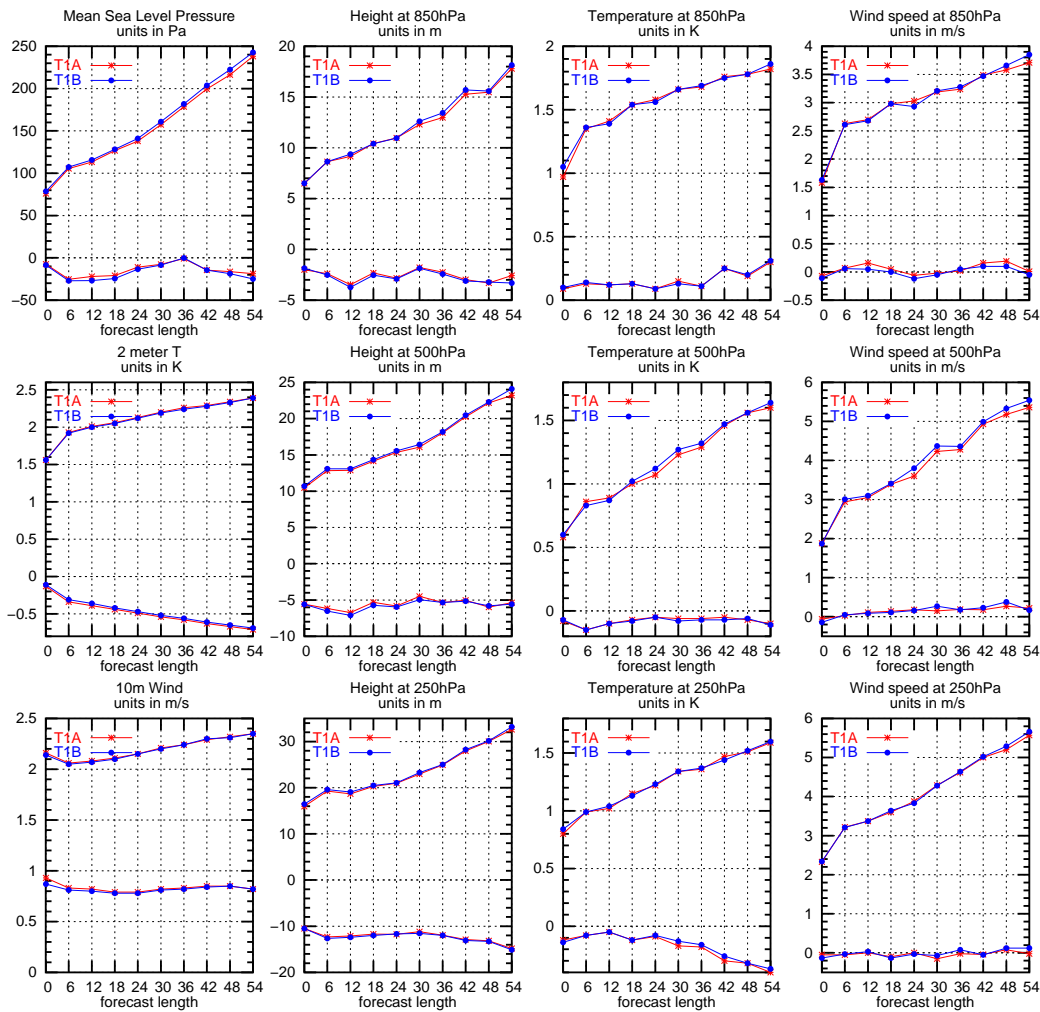


Figure 5: Observation verification scores of key parameters averaged for forecasts with 3D-VAR analysis using a) interpolated SMHI 31-level background error structure functions, with a scaling factor of 0.4 for p_s , u_{ag} , v_{ag} and T , and 0.6 for Q , (in red), and b) T15 structure functions with a scaling factor of 0.6 for p_s , T , Q and 0.3 for u_{ag} and v_{ag} . The test period is between Jan 5 and Jan 15, 2005. Note the forecast system used in this test is DMI-HIRLAM-T15.

Assimilation of AMV wind

Several impact studies (unpublished results) with the DMI-HIRLAM analysis and forecasting system have in the past shown a very clear negative impact of using SATOB (Satellite Observations (WMO data code for satellite cloud wind data)) data. However, the latest impact study of this kind of data was made around 2000 and a lot of progress in the production of these data has been made by the satellite data providers (see, e.g., the proceedings from “The Seventh International Winds Workshop” available from <http://www.eumetsat.int/>). In addition, the new instrument SEVIRI (Spinning Enhanced Visible and Infrared Imager) on Meteosat-8 has also made it possible to further improve the assignment of wind compared to wind data from the older meteosat satellites. The data are now provided in bufr-code directly from EUMETSAT via EUMETCast. The first tests at DMI showed that the comparison of the AMV with first guess fields showed similar or better statistics than similar comparisons of the radiosonde wind data. Accordingly, the original observation error standard deviations (σ_o) for SATOB winds, that were somewhat higher than the corresponding radiosonde wind error standard deviations, were reduced to being comparable to the radiosonde

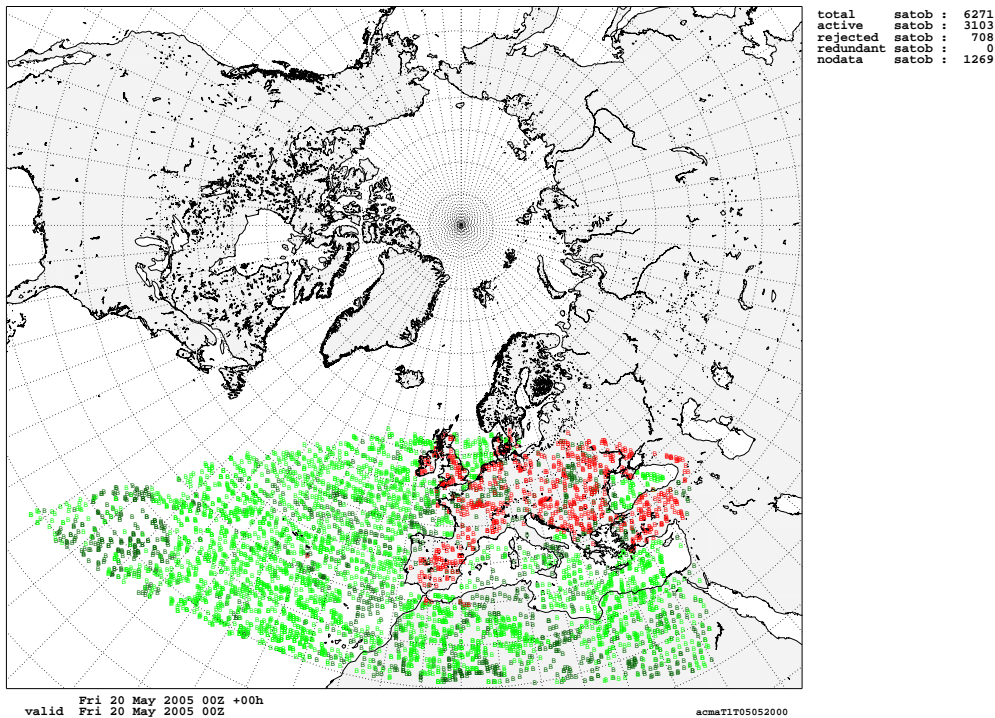


Figure 6: Use of Meteosat-8 AMV data for cycle 2005052000 in the new DMI-HIRLAM-T15.

wind error standard deviations. Table 1 shows these.

An example of the 00 UTC data coverage during the pre-operational test period is given in Figure 6. Note that the number of available data is higher during daytime due to data derived from the SEVIRI spectral channels in the visible range.

The AMV data includes two quality indices and as a first order rejection (in the obsproc programme) the data are rejected if the quality indices are below 20 or 30, respectively. The first guess check in the analysis of Meteosat-8 AMV data (and other single level wind data) is traditional and includes an “asymmetry check” (see Geijo & Amstrup, 2005). AMV data over land north of 30°N are rejected in accordance with tradition. Further tests need to be made before including these data.

Figure 7 demonstrates results of a parallel data assimilation test for a three week period in Jan 2005 using DMI’s previous operational suite, DMI-HIRLAM-GEDN, in which the control setup is compared to the one including use of AMV wind data. A slightly positive impact on upper air scores for geopotential height and wind can be identified from the figure.

Multinode 3D-VAR analysis with MPI

Experiments have been made to utilize multiple nodes on the NEC-SX6 platform for the 3D-VAR analysis, in order to accommodate the need for assimilating increasingly larger amounts of observation data. This involves a change of parallelization strategy from the previous OpenMP to that with message passing (MPI), the latter being the only feasible way of data communication on the multinode NEC SX6 platform. At the moment the total execution time for a 3D-VAR analysis on T15 domain is around 5 min using 3 nodes, comparable to the time needed on single node using OpenMP with the previous 3D-VAR suite. It is estimated that further tuning of configuration parameters concerning observation handling in 3D-VAR may potentially result in faster execution.

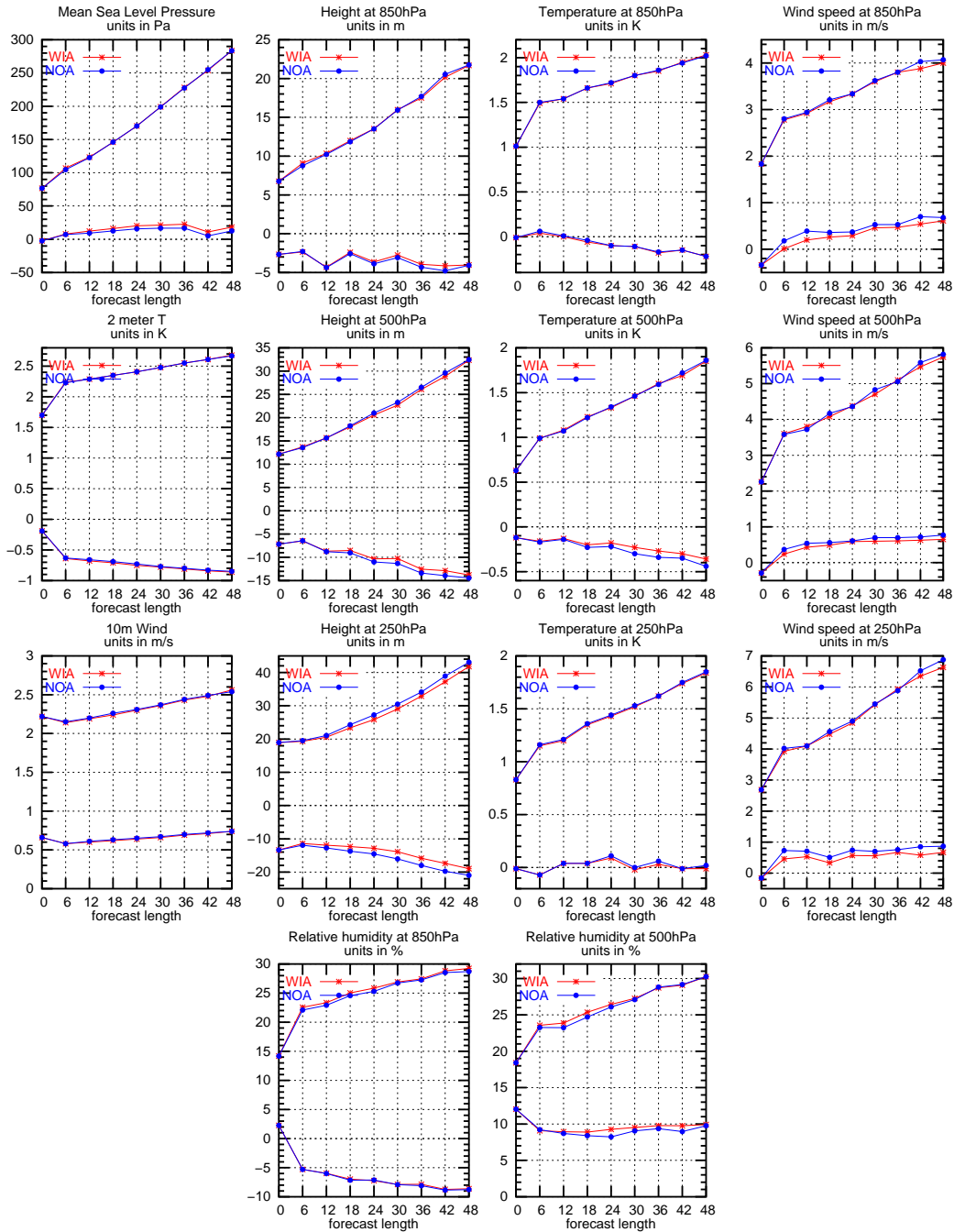


Figure 7: Observation verification scores (rms and bias) validated against the EWGLAM-station list for parallel runs comparing DMI-HIRLAM-E15 runs with AMV data (in red) and without AMV data (in blue), for the period 20050101 to 20050125.

Forecast model

Several changes have been introduced into the forecast model, both in terms of upgrades in the basic dynamic core and tuning of physical parameterization.

SETTLS scheme

For the dynamics part, the SETTLS (Stable Extrapolation Two-Time-level Scheme, Hortal, 1998) has been implemented for calculation of the non-linear terms of the evolution equations. The scheme has been introduced earlier, successfully, into the forecast system like IFS at ECMWF. With SETTLS, instead of extrapolating the non-linear values to time level $N+1/2$, the values are

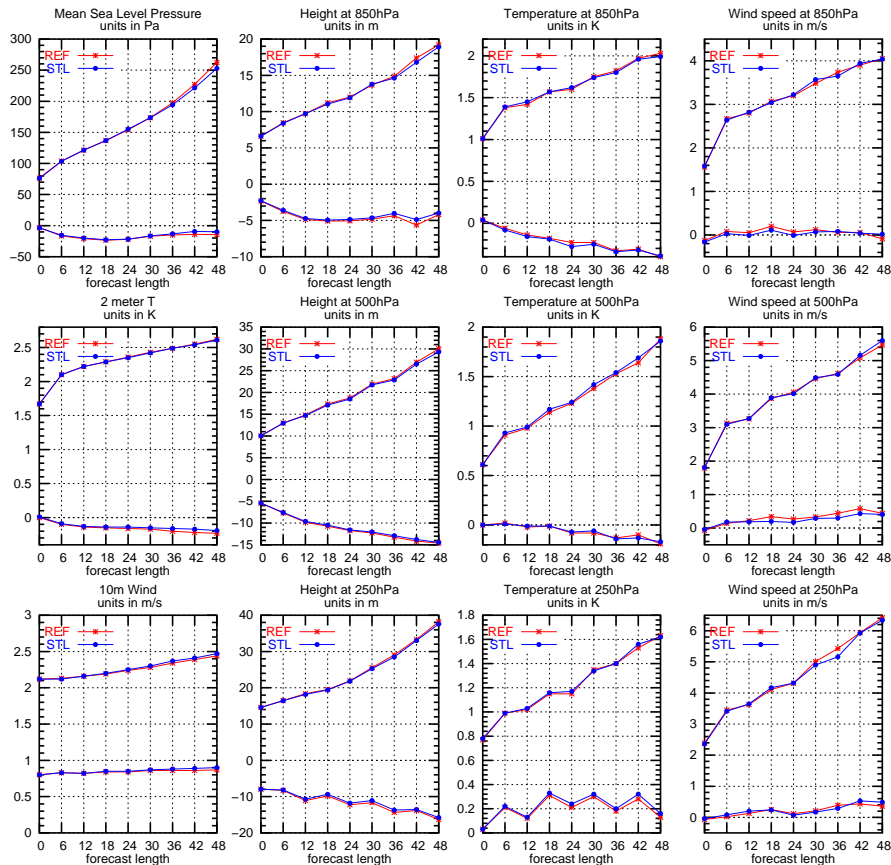


Figure 8: EWGLAM observation verification of key parameters, in rms and bias, averaged for forecasts using a) reference HIRLAM 6.3.7 (without the SETTLS), with stars and labeled as REF and b) with SETTLS, with circles and labeled STL. The test period is 14-28 of November 2004, using RCR with 0.2 degree resolution and $\Delta t = 450$ s.

estimated at time level n and $n-1$ using the departure point of the semi-Lagrangian trajectory corresponding to the present time step when determining values N^n and N^{n-1} (see equation (3) in Lindberg (2005)). In that calculation, only the arrival and departure points of the present trajectory are used, hence the method is compatible with the semi-implicit treatment of the linear terms of the evolution equations. This scheme is therefore stable according to linear stability analysis. The details of the scheme and its implementation in HIRLAM can be found in Lindberg (2005).

The SETTLS scheme can be activated through a new namelist variable NLSETTLS in the namelist NAMRUN. When set to true, the SETTLS scheme is used to calculate the non-linear terms, otherwise the non-linear terms are calculated as in the present HIRLAM version. The required code modification is limited, including those in the subroutines SL2TIM and SLDYNM. In SL2TIM, the routine COMPFX is called with `ICALL = 1` for NLSETTLS being true, which means that all fields are just passed into new arrays through this routine whereas for NLSETTLS being false (the current default in Reference HIRLAM) it is called with `ICALL = 2`, which means all fields are extrapolated to time level $N+1/2$ in COMPFX. For NLSETTLS being true the subroutines COMPFX and SLDYN are called twice (for all values in time-level n and time-level $n-1$). In the latter subroutine the non-linear terms are evaluated. Since there are now two time-levels involved in calculation of the non-linear terms, an extra set of arrays for all variables at time-level $n-1$ is assigned and modified by horizontal diffusion before being passed into SLDYNM (where these new values are also passed). The assignment of the new namelist variable NLSETTLS involves changes in NAMEIN.f and COMHQP.inc.

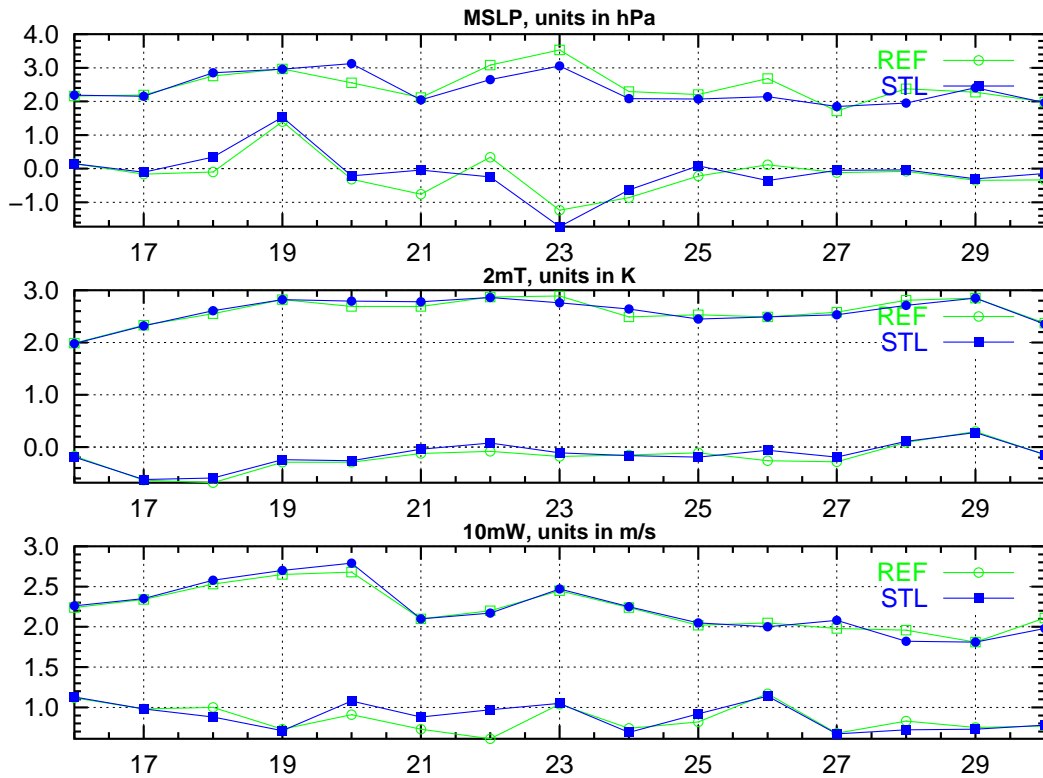


Figure 9: Daily averaged std and bias for MSLP, 2 m temperature and 10 m wind in 48 h forecasts for the period 14-28 of November 2004 for the EWGLAM stationlist. The curves with open circles are for the reference 6.3.7, those with closed squares are for the SETTLS run.

Figure 8 shows observation validation of the SETTLS scheme implemented on top of the reference HIRLAM version 6.3.7 on the IBM computer at ECMWF. A 2 week period from 14 to 28 of November 2004 was chosen. The period features some high wind situations, during which the operational DMI-HIRLAM has been seen to be noisy. From the figures, the verification scores with and without the SETTLS schemes in the non-linear terms look rather similar, with the one using SETTLS showing a small improvement for forecasts longer than 36 hours. Figure 8 shows the daily averaged errors for three surface parameters MSLP, 2 meter temperature and 10 meter wind, in which the SETTLS runs again show some marginally better scores. SETTLS runs have also been seen to result in a reduction of the noise level (not shown). Finally the computational cost associated with SETTLS is quite similar to the control run. For DMI-HIRLAM, it is observed that the runs with SETTLS scheme are merely approximately 2% slower than the control runs for a 60 h forecast. Although further tests and case studies to investigate the performance of the SETTLS scheme for various flow conditions could be desirable, it is felt that a stable behavior and marginally positive results under high wind conditions as shown in the above tests is sufficient to justify an operational implementation.

Changes in physical parameterization

Several changes have been implemented in the physical parameterization, involving components in convection, turbulence, radiation and near surface scheme. For the cloud and condensation scheme using STRACO (Sass, 2002), the following modifications have been made on top of the version used in Reference 6.3:

- New convective cloud cover formulation based on a 3-box rectangular (asymmetric)

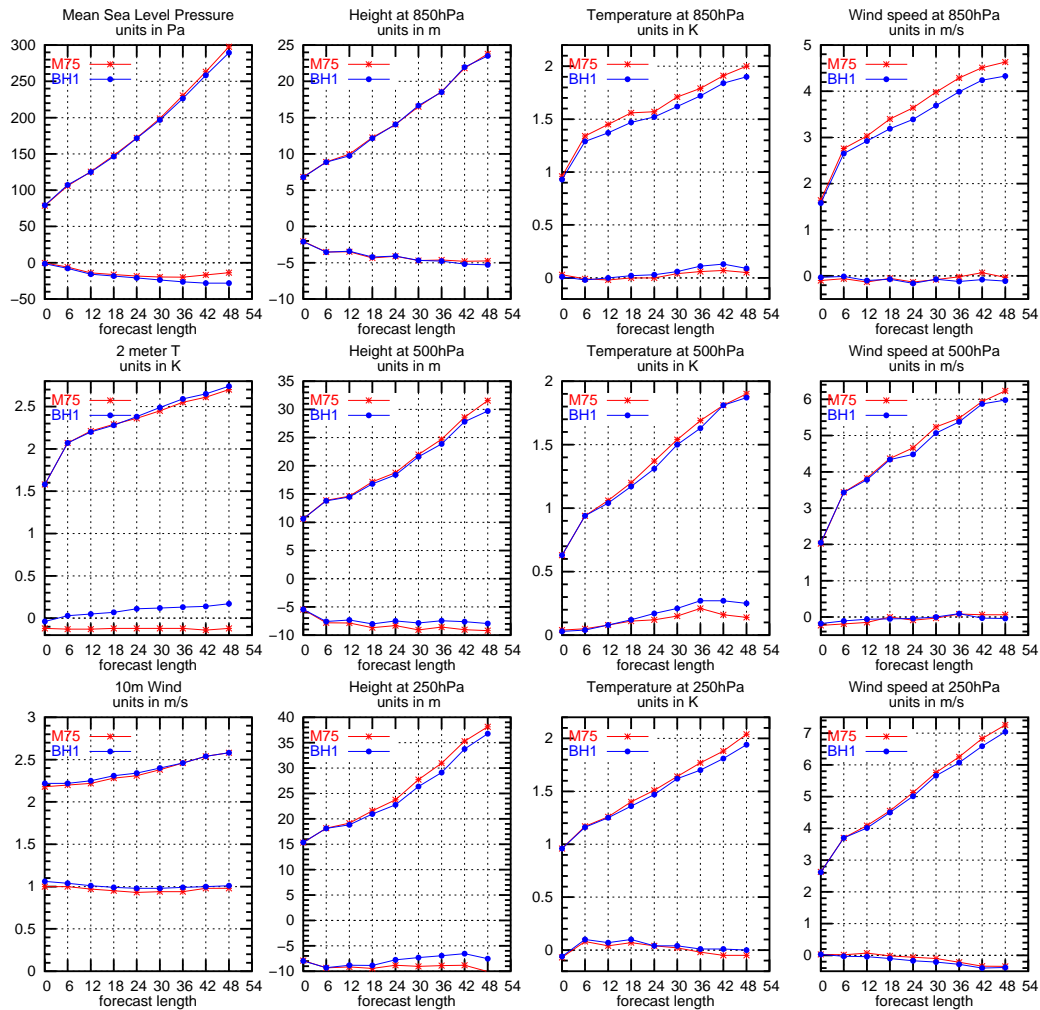


Figure 10: Observation verification scores of key parameters averaged for forecasts using a) reference 6.3.6 (in red) and b) with tuning of turbulence (CBR) and condensation (STRACO) schemes. The test period is for Jan 15 to 31, 2002 using reference RCR domain at 0.2 degree resolution.

probability function for the total specific humidity. The basic scheme has been successfully tested during the development phase by 1D model simulations with dynamical forcing adequate for cases of convective boundary layers. These have been studied in the literature using large-eddy simulations (for BOMEX, ASTEX, EUROCS cases).

- Tuning of a precipitation release parameter for convective clouds, simulating indirectly the effect of different aerosol distributions over land and sea, respectively, implying different cloud droplet size distributions. As a consequence, convective clouds need to be thicker over land compared to sea before significant precipitation release. This effect is introduced through the dependency of a precipitation release parameter on the land fraction in the model grid.
- A dependency on model resolution of the moistening parameter connected to water vapor entering convective clouds without condensing. This modification is based on studies in the literature of the water budget components of small convective storms.
- A slight tuning of the convective cloud entrainment model.

Table 2: Contingency table, 2002011500-2002013106

6.3.6 12-24 h							MOD 12-24 h						
	O1	O2	O3	O4	O5	sum		O1	O2	O3	O4	O5	sum
F1	3579	165	68	12	2	3826	F1	3964	217	63	11	3	4258
F2	1666	534	275	32	10	2517	F2	1359	497	291	32	6	2185
F3	607	565	956	216	61	2405	F3	536	558	933	221	61	2309
F4	41	43	165	189	66	504	F4	35	34	178	188	83	518
F5	7	4	32	46	71	160	F5	6	5	31	43	57	142
sum	5900	1311	1496	495	210	9412	sum	5900	1311	1496	495	210	9412
%FO	61	41	64	38	34	57	%FO	67	38	62	38	27	60

636 24-36 h							MOD 24-36 h						
	O1	O2	O3	O4	O5	sum		O1	O2	O3	O4	O5	sum
F1	3429	194	87	13	5	3728	F1	3821	240	79	7	5	4152
F2	1561	517	320	49	13	2460	F2	1238	476	342	62	10	2128
F3	640	506	894	220	62	2322	F3	577	512	850	213	60	2212
F4	39	49	134	159	75	456	F4	33	36	169	163	73	474
F5	11	7	32	40	54	144	F5	11	9	27	36	61	144
sum	5680	1273	1467	481	209	9110	sum	5680	1273	1467	481	209	9110
%FO	60	41	61	33	26	55	%FO	67	37	58	34	29	59

- Removal of a small inconsistency in the treatment of evaporating precipitation for small precipitation rates.
- A slight tuning of the mixing length formulation in the turbulence scheme as a result of other modifications in the model. This is performed in view of the strong link between the turbulent and convective transport.
- Correction of a bug in the cloud absorption of solar radiation which was previously underestimated.

The above modifications were implemented first in the reference HIRLAM 6.3.6 and tested on the ECMWF computer platform, HPCD, for two half-month episodes in winter and summer, respectively, using the reference HIRLAM Regular Cycle of Reference system (RCR) configuration. The main benefit of the tuning is reflected in the improvement of the forecast for the lowest class precipitation events (none-or-low) in both periods, see Table 2 and Table 3. Figure 10 and Figure 11 show the observation verification of key parameters comparing the reference HIRLAM and the tuned turbulence and condensation schemes, for the episodes in Jan 2002 and June 2002, respectively. For both periods, the modification resulted in a small drift of T2m bias, from negative to positive, and improvement in rms scores of the lower troposphere wind and temperature.

In addition, the proposed modification by Sander Tijm, KNMI on the surface scheme to improve dew point temperature, (Tijm, 2005), has also been implemented in the updates. In this modification, the prescribed values of the leaf area index and vegetation index for the cropland vegetation type have been modified. Apart from an increase in minimum values, an interpolation scheme is introduced to change monthly values of the above quantities to slowly changing daily values. More details can be found in Tijm (2005).

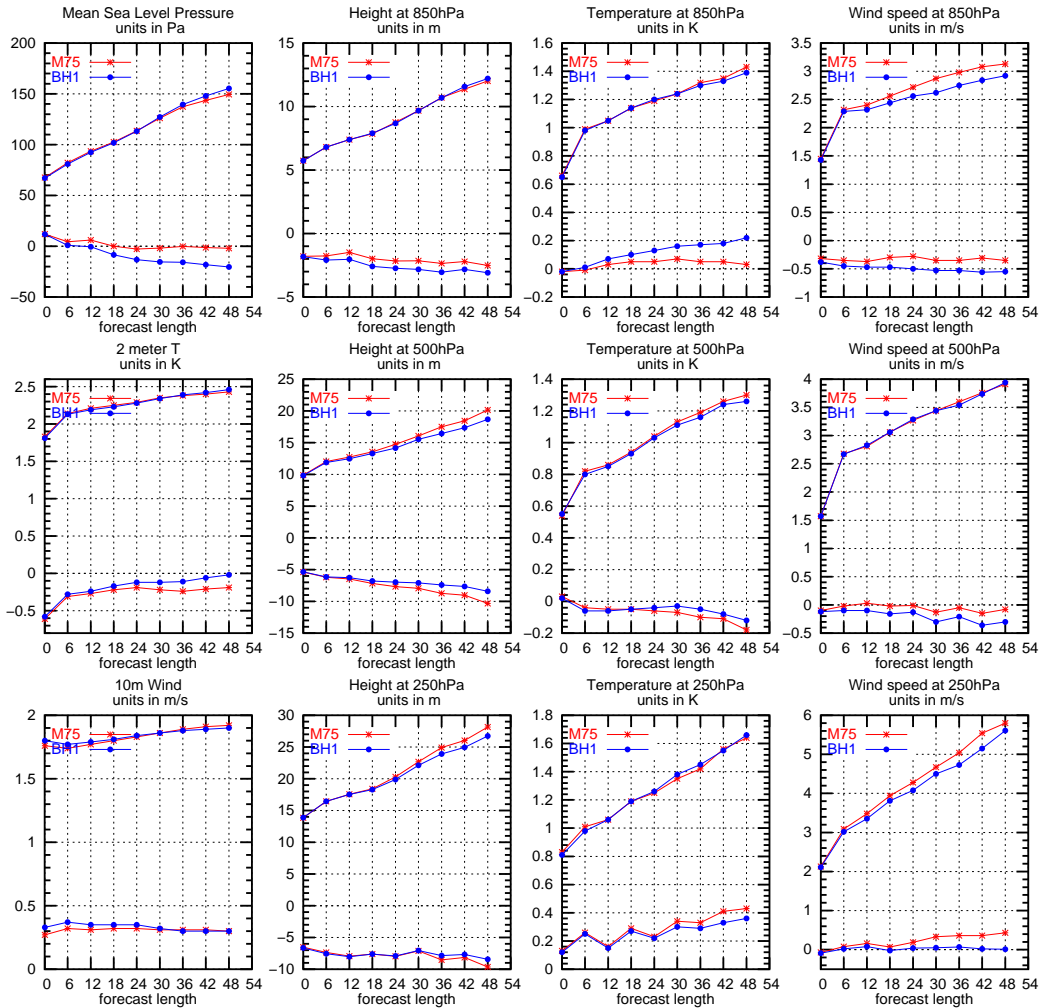


Figure 11: same as in Figure 10 but for the summer period between June 10 and June 24, 2002.

Summary

Based on extensive data assimilation tests of individual components as described in this note, a combined upgrade suite was assembled. In summary, the update includes the following new features:

- For the surface analysis module, the SST data from OSI-SAF are assimilated, using a thinning distance of 20 km. The surface analysis now is performed on eight processors using OpenMP parallelization;
- For the upper air analysis, a reduced scaling of ca. 0.4 for the background error structure function is used, thus increasing the weight for model data in the assimilation. The 3D-VAR analysis is run on multiple NEC-SX6 nodes using MPI parallelization, replacing the previous OpenMP parallelization which is only feasible on a single node;
- The Meteosat-8 Atmospheric Motion Vector (AMV) data are now assimilated in the form of a type of SATOB data;
- For the forecast model, the SETTLS option in the semi-Lagrangian scheme is implemented. A series of tunings in the physical parameterization (CBR turbulence scheme, STRACO

Table 3: Contingency table, 2002061000-2002062418

636 12-24 h							MOD 12-24 h						
	O1	O2	O3	O4	O5	sum		O1	O2	O3	O4	O5	sum
F1	5140	191	92	29	23	5475	F1	5306	163	70	20	16	5575
F2	1015	196	185	36	21	1453	F2	856	202	175	40	27	1300
F3	475	217	312	113	87	1204	F3	469	246	342	119	79	1255
F4	50	35	74	55	44	258	F4	52	32	76	52	58	270
F5	20	13	28	31	37	129	F5	17	9	28	33	32	119
sum	6700	652	691	264	212	8519	sum	6700	652	691	264	212	8519
%FO	77	30	45	21	17	67	%FO	79	31	49	20	15	70

636 24-36hr							MOD 24-36hr						
	O1	O2	O3	O4	O5	sum		O1	O2	O3	O4	O5	sum
F1	5072	197	120	31	24	5444	F1	5189	186	98	28	23	5524
F2	861	177	162	49	35	1284	F2	787	167	159	40	25	1178
F3	502	198	270	95	65	1130	F3	463	218	306	97	76	1160
F4	60	31	58	44	40	233	F4	52	32	63	53	42	242
F5	11	10	30	33	36	120	F5	16	10	14	34	34	108
sum	6506	613	640	252	200	8211	sum	6507	613	640	252	200	8212
%FO	78	29	42	17	18	68	%FO	80	27	48	21	17	70

condensation scheme, near-surface parameterizations) have been implemented. A bug fix has been made for the radiation scheme.

In the final stage of the upgrade, validation experiments have been performed for three periods, each about one month long. Two of these periods are historical episodes, one for winter, Jan 5 to Feb 5, 2005, and another for summer, July 1 to Aug 31, 2004. The third period, from May 1 to May 28, 2005, is a real-time parallel test in which the new and the operational suites have been tested with identical conditions. In the accompanying report (Kmit et al., in preparation), we summarize results of these validation runs including some individual case studies. These results show generally a significant improvement in observation verification scores of main parameters, notably those for screen level temperature and humidities and to a certain extent the rms of MSLP and upper air parameters. The upgrade also brings some improvement in the precipitation forecast, notably for the small (or none) precipitation class.

In addition to the above described updates, a new Greenland model, DMI-HIRLAM-Q05, at a grid-spacing of 0.05 degree (ca. 5.5 km) and covering the southern part of Greenland, is officially put into the operational suite. The model configuration is similar to that of S05, in which no upper air data assimilation is performed. A surface analysis is made for Q05, which, together with the T15 analysis valid at the same time, is used to initiate the forecast. More details about the model can be found in Korsholm et al. (2005).

In view of the positive validation results from parallel experiments, the upgrade was formally launched on May 31, 2005.

Acknowledgment

Sander Tijm, KNMI, kindly provided the source code modification to improve the prediction of surface dew point temperature. The work with re-scaling of background error structure functions has

benefited from discussions with other HIRLAM colleagues, especially Nils Gustafsson (SMHI), Magnus Lindskog (SMHI) and Ole Vignes (met.no).

References

Geijo Guerrero, C. and B. Amstrup, 2005: Assimilation of M8-AMV data in the HIRLAM-NWP model. *Hirlam Newsletter*, **49**, 12-21.

Gustafsson, N., L. Berre, S. Hörnquist, X.-Y. Huang, M. Lindskog, B. Navascués, K. Mogensen and S. Thorsteinsson, 2001: Three-dimensional variational data assimilation for a limited area model. Part I: General formulation and the background error constraint. *Tellus*, **53A**, 425-446.

Hortal, M., 1998: Some recent advances at ECMWF. *LAM News*, **27**, 32-36.

Korsholm, U., C. Petersen and M. Kmit, 2005: High resolution DMI-HIRLAM model covering southern Greenland. *DMI Technical Report*, **05-02**.

Lindberg, K., 2005: The effects of the modifications aimed to reduce noise in the semi-Lagrangian scheme in DMI-HIRLAM and the first preliminary tests of the SETTLS scheme in HIRLAM. *HIRLAM Newsletter*, **48**, 128-134.

Lindskog, M., 2000: An estimation of the seasonal dependence of background error statistics in the HIRLAM 3D-Var. *HIRLAM Newsletter*, **35**, April 2000, 71-86.

Navascués, B., M. Lindskog, X. Yang and B. Amstrup, 2006: Diagnosis of error statistics in the HIRLAM 3D-VAR. *HIRLAM Technical Report*, **66**.

Sass, B. H., 2002: A research version of the STRACO cloud scheme. *DMI Technical Report*, **02-10**, pp 27.

Tijm, S. 2005: Problems with the HIRLAM dew point temperature. *HIRLAM Newsletter*, **48**, 92-98.

Yang, X., C. Petersen, B. Amstrup, B. Andersen, H. Feddersen, M. Kmit, U. Korsholm, K. Lindberg, K. Mogensen, B. H. Sass, K. Sattler and N. W. Nielsen, 2005: The DMI-HIRLAM upgrade in June 2004. *DMI Technical Report*, **05-09**, pp 34.

Appendix: Operational schedule

Table 4: Operational schedule of DMI-HIRLAM which lists regular launch times for T15, S05 and Q05 runs. T_E in the table denotes a re-forecast initiated with the ECMWF analysis and first guess of T15.

Launch Time (UTC)	T15 Cycle	S05 Cycle	Q05 Cycle
01:37	T00 +60 h		
02:20		S00 +54 h	
03:00			Q05 +36 h
ECMWF-BC 00 UTC			
07:37	T06 +60 h		
08:20		S06 +54 h	
ECMWF-BC 06 UTC			
11:45	T_E00 +05 h		
	T03 +05 h		
	T06 +05 h		
	T09 +05 h		
13:37	T12 +60 h		
14:20		S12 +54 h	
15:00			Q05 +36 h
ECMWF-BC 12 UTC			
19:37	T18 +60 h		
20:20		S18 +54 h	
ECMWF-BC 18 UTC			
23:45	T_E12 +05 h		
	T15 +05 h		
	T18 +05 h		
	T21 +05 h		



Contact

For more information please contact xiaohua@dmi.dk or kmit@dmi.dk.

Previous reports

Previous reports from the Danish Meteorological Institute can be found at:
<http://www.dmi.dk/dmi/dmi-publikationer.htm>